④ 対向照射法を用いて，線量分布の部位による差異が5%以下になるようにすべきである。

[2] 骨盤照射

全腹部照射に引き続き，骨盤部に限局した照射を追加し(追加線量は20 Gy程度)，骨盤部の総線量を45～50 Gyとする。しかし，骨盤部追加照射は意義がないとする報告もある[19]。骨盤部の照射法は子宮頸癌を参照されたい(図1，2)。

治療成績

放射線治療単独の成績はなく，また，補助療法としての価値も不明瞭である。参考として，術後全腹部照射や骨盤部の照射を行った成績を表9に示した。

■ 表9. 骨盤単独と全腹部骨盤照射の比較

報告者	臨床期(残存腫瘍)	照射		再発			5年生存率
		全腹部	骨盤部	骨盤部	上腹部	骨盤＋上腹	
Schray	None	−	50～60 Gy	0/36	7/36	0/36	82%
	<2 cm	−	50～60 Gy	2/26	5/26	2/36	52%
Dembo	I, II, III	22.5 Gy	45 Gy	0/50	0/50	11/50	78%
	micro	−	45 Gy	0/31	8/31		47%
Delclos	II	28 Gy	48 Gy	?	?	25/38*	35%
			50 Gy	?	?	14/17*	18%
Perez	II	28 Gy	50 Gy	0/17	1/17	4/17	57%
			50 Gy	2/14	1/14	4/14	16%

* 再発部位が骨盤・上腹部に分けて記載されていないため，仮に骨盤＋上腹部に分類した。

有害事象と対策

全腹部照射を行った場合，有害事象として以下のことが報告されている。Fylesらは，初回治療としてWARを行った598例の有害事象を報告した[21]。早期有害事象として，悪心・嘔吐，下痢，白血球減少，血小板減少である。23%で治療を中断する必要があり，10%は骨髄抑制のため完遂できなかった。晩期障害は慢性下痢，一時的肝酵素上昇，症状のある下肺野の肺臓炎，小腸閉塞であった。

4. 腟癌

はじめに

腟癌は閉経期以降の50～70歳代に多く発生し，種々の内科的合併症をもつ頻度も高い。また腟は膀胱，直腸に近接し容易に直接浸潤を起こすため，根治的手術が容易でない。し

たがって，放射線療法が根治的治療として用いられことも多い。しかし，卵巣機能を温存したい場合や，上皮内癌や疣贅癌では手術が積極的に行われる。

腟癌は婦人科腫瘍の1～2% 以下である。本項では他の施設の治療法を参照し，予後因子として最も重要な臨床病期(FIGO 分類)に従って放射線治療の方針述べる。腟上部に発生した腟癌は，基本的に子宮頸癌に準じて治療する。

病理分類

大部分(90% 以上)は扁平上皮癌である。腺癌の場合は大部分転移性(子宮体癌からの転移が多い)であるが，腺組織がないにもかかわらずまれに原発性腺癌もある。その他，5歳以下の小児に好発し，ぶどうの房に類似した多房性ポリープを呈する横紋筋肉腫(ぶどう状肉腫)や，悪性黒色腫も発生する。

病期分類

一般に FIGO 分類(1974 年)が使用されるため，これを表 10 に示した。

■ 表 10. 腟癌進行期分類(FIGO, 1974 年)

進行期	
0 期	上皮内癌
I 期	癌が腟壁に限局するもの。
II 期	癌が腟壁下に広がるが，骨盤壁には達していないもの。
III 期	癌が骨盤壁に達しているもの。
IV 期	癌が小骨盤を越えているか，あるいは臨床的に膀胱・直腸の粘膜を侵しているもの。 (注：胞状浮腫だけでは IV 期に入れない)
IVA 期	近位の他臓器に広がるもの。
IVB 期	遠隔臓器に広がるもの。

治療方針

治療方針の例としてマリンクロット研究所の治療方針を示す[22]。根治的放射線療法は初期の腟癌を腔内照射単独で治療し，進行癌には外照射と腔内照射を併用する。

① 0-I 期：腔内照射単独で腫瘍に 65～80 Gy 照射するが，腟癌は多中心性に発生することも多く，50～60 Gy を腟粘膜表面全体に照射しておく。腟癌の治療に用いるアプリケータは，病巣の位置に合わせて適宜変更する。I 期の浸潤性で分化度の低い腫瘍には外照射と腔内照射を組み合わせる。

② II 期：II 期は骨盤リンパ節転移が 25～30% に存在すると報告されており[23]，リンパ節領域への外照射が併用される。外照射 45～50 Gy 後(20～30 Gy で中央遮蔽)，腔内照射と組織内照射で腫瘍部へさらに 45～55 Gy 照射する。

③ III・IVA 期：外照射を 50～55 Gy 行い，40 Gy 以後は中央遮蔽を挿入する。腔内照

射または組織内照射で 20～25 Gy を腫瘍部に追加する。

IVB 期：対症療法として放射線治療を行う。出血や疼痛には 40～50 Gy 照射する。

治療方法

腟癌の放射線治療は基本的に根治的治療となる。

a. 外照射

外照射は基本的には子宮頸癌に準じて行う(図 1，2)。腟癌の外照射で気をつける点は，腫瘍の存在部位により照射範囲を変える必要がある。腟の上部 2/3 はリンパ節転移が腸骨領域のみで，通常の骨盤照射でよい。下 1/3 は大腿部と鼠径部への直接転移がある。そのため，通常の骨盤照射より下方が広い照射野となる(図 8)。全骨盤照射と鼠径部のみを電子線で照射する方法もある。

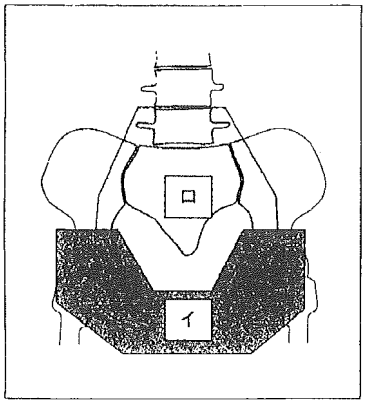

■ 図 8. 腟癌・外陰癌の外照射の照射野(骨盤部)
腟の上方に発生した腟癌は子宮頸癌と同様に全骨骨盤の照射野(ロ)で，2 Gy×25-30 回 50 60 Gy 照射する。腟下方に発生した腟癌と外陰癌は，原発巣を十分含めるとともに，鼠径リンパ節への転移が多発するため，腸骨リンパ節(ロ)とともに鼠径リンパ節(イ)も照射する。照射線量は骨盤部とともに(イ＋ロの照射野)，2 Gy×25-30 回 50-60 Gy 照射する。腟下方および外陰の初期癌では(イ)のみの照射でよい。

b. 腔内照射

一般には子宮頸癌の治療法に準じるが，円筒型のアプリケータかオボイドを用いる。腟円蓋部や腟の上部に病変が存在する場合は円筒形のアプリケータでは線量が低下する危険があり，オボイドを 2 本挿入するほうがといと思われる。腫瘍の分布によっては，子宮頸癌の腔内照射に用いるタンデムとオボイドを使用することで良好な線量分布が得られる場合もある。モールドで個々の腟の形に合わせたアプリケータを作成するのも 1 つの方法である。腫瘍の浸潤が深い場合や傍子宮結合織への浸潤が強い場合は，腔内照射と組織内照射を併用することによって良好な線量分布を得ることが可能である。高線量率腔内照射は子宮頸癌と同様に 1 回 5 Gy を週 1 回，4 回治療するという施設もあれば[24]，1 回 3～8 Gy で 2 週に 1 回，総線量 21 Gy というスケジュールをとっている施設もある[25]。腟癌の腔内照射は患者が少なく確立した方法がない。

c. 組織内照射

病変が小さく浅いものでは ^{198}Au グレインの永久刺入も可能であるが，一般には ^{137}Cs 針や ^{226}Ra 針が使用された。^{192}Ir 後充填を用いた高線量率組織内照射も行われているが，

最適な分割方法や照射線量についてはまだ確立されていない。さらに，高線量率(HDR)と低線量率(LDR)の両者の利点を取り入れた方法で組織内照射を行っている施設もある(Pulsed HDR)[26]。

治療成績

放射線治療単独の治療成績を図9に示す[22]。

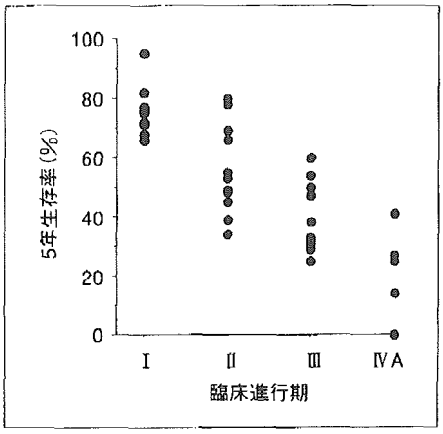

■図9. 腟癌根治的放射線治療による5年生存率

有害事象と対策

骨盤部の照射の有害事象として子宮頸癌の項を参照されたい。

5. 外陰癌

はじめに

外陰癌は婦人科癌のなかで3～4%を占め，主に高齢者に多く見られる。外陰癌は初期癌，浸潤癌のいずれも治療の第一選択は手術であるが，高齢者に多い疾患で，様々な内科的疾患のために手術適応とならない例も多い。浸潤癌には両側鼠径リンパ節摘出が必要である。クリトリスや前庭部に病変がある場合は，腸骨リンパ節郭清も必要であるが，手術の代わりに照射することも考えられる[27]。

病理分類

外陰癌の90%は扁平上皮癌である。その他に基底細胞癌，腺組織由来のPaget's disease やバルトリン腺癌，悪性黒色腫などがある。

病期分類

一般にFIGO分類が使用され，表11に示した。

■ 表 11. 外陰癌進行期分類(FIGO, 1994)

進行期	
I	外陰または会陰に限局した最大径 2 cm 以下の腫瘍(T 1)。リンパ節転移はない(N 0)。
IA	外陰または会陰に限局した最大径 2 cm 以下の腫瘍で，間質浸潤は 1.0 mm 以下のもの*。リンパ節転移はない(N 0)。
IB	外陰または会陰に限局した最大径 2 cm 以下の腫瘍で，間質浸潤は 1.0 mm 以上のもの。リンパ節転移はない(N 0)。
	* 浸潤の深さは隣接した最も表層に近い表皮に近い真皮乳頭の上皮間質接合部から浸潤先端までの距離とする。
II	外陰および/または会陰に限局した最大径 2 cm を超える腫瘍(T 2)。リンパ節転移はない(N 0)。
III	腫瘍の大きさは問わず，(1)隣接する下部尿道および/または腟または直腸に進展するもの，および/または，(2)片側の所属リンパ節転移があるもの。
IVA	腫瘍が次のいずれかに浸潤するもの：上部尿道，膀胱粘膜，直腸粘膜，骨盤骨，および/または両側所属リンパ節転移があるもの。
IVB	骨盤リンパ節を含むいずれかの部位に遠隔転移があるもの(M 1)。

治療方針

外陰癌における根治的治療としての放射線治療の役割は，いまだ確立していない。外陰癌に対する放射線治療の役割としては，根治的放射線治療のほかに，早期病変に対しての縮小手術との組み合わせ，臨床的にリンパ節転移陰性症例に対するリンパ節郭清の代わりとしての領域リンパ節への照射，進行期症例に対する術後照射，手術困難な症例に対して腫瘍量を減少させるための術前照射，出血，疼痛などに対する姑息的照射などが挙げられる。

例数も少なく対象が進行癌ではあるが，化学療法と放射線治療の同時併用により比較的期待のもてる結果が報告されている[28]。併用される薬剤としては MTX, 5-FU, CDDP, MMC, BLM などであり，照射線量としては 30～50 Gy 程度が選択されることが多いようである。

治療方法

[1] 根治的放射線治療

a. 外照射

小さい表層性の原発病変には 60～65 Gy の外照射あるいは組織内照射を行う。大きい腫瘍に対しては外陰部と所属リンパ節を含めて 45～50 Gy 照射後，適切なエネルギーの電子線，低エネルギーの X 線あるいは組織内照射で 10～20 Gy 追加し，総線量 65～70 Gy を照射する。

骨盤部リンパ節も照射する場合，下縁は会陰部が完全に含まれるようにする(図 8 イ，

ロ)。いずれの照射野の場合も，45～50 Gy 後は原発巣あるいは鼠径リンパ節に限局した照射野に変更する(図 8 イ)。

b. 組織内照射

病巣が小さく表在性であれば ^{198}Au グレインによる照射を行う。浸潤の深い病変に対しては ^{192}Ir ワイヤーによる照射を行う。

［2］術前照射

進行癌のため手術が不可能あるいは困難な症例は，照射で腫瘍を縮小させた後に手術を行う場合がある。

［3］術後照射

根治的切除術を受けたが，切除断端が不十分な場合，鼠径部リンパ節に転移が陽性であった場合，原発巣のみを切除された場合などは 50 Gy 程度の術後照射の対象となる。

［4］姑息照射

出血，疼痛などに対しては 40～50 Gy の照射を行う。

治療成績

本邦の全国集計では 5 年生存率が I 期 66.7%，II 期 41.2%，III 期 34.3%，IV 期 28.6% と手術と比べて遜色ない結果が報告されている。根治的放射線治療成績は臨床進行期ごとにまとめて図 10 に示した。

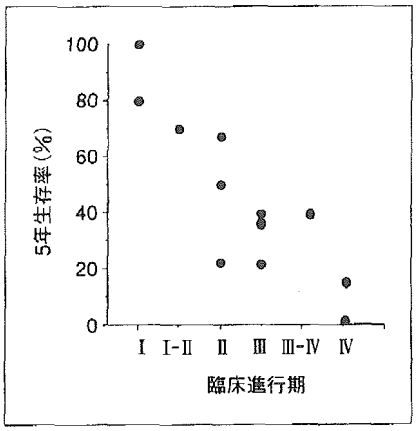

■ 図 10. 外陰癌放射線治療による 5 年生存率

有害事象と対策

子宮頸癌の項を参照されたい。外陰癌の治療で特徴的なことは，外陰部の皮膚に大線量が照射されるため，皮膚炎が重症になることである。

(伊東久夫，宇野　隆，川田哲也)

文 献

1) Eifel PJ et al : Cancer of the Cervix, Vagina, and Vulva. Cancer : Principles and Practice of Oncology. Ed. DeVita VT Jr et al, Philadelphia ; Lippincott-Raven, 1997 : 1433-1462.
2) Rose PG et al : Concurrent cisplatin-based radiotherapy and chemotherapy for locally advanced cervical cancer. N Engl J Med 1999 ; 340 : 1144-1153.
3) Whitney CW et al : Randomized comparison of Fluorouracil plus cisplatin versus Hydoroxyurea as an adjunct to radiation therapy in stage IIB-IVA carcinoma of the cervix with negative para-aortic lymph nodes : A Gynecologic Oncology Group and Southwest Oncology Group Study. J Clin Oncol 1999 ; 17 : 1339-1348.
4) Pearcey R et al : Phase III trial comparing radical radiotherapy with and without cisplatin chemotherapy in patients with advanced squamous cell cancer of the cervix. J Clin Oncol 2002 ; 20 : 966-972.
5) 伊藤久夫：子宮頸癌の放射線療法－他施設間での比較－．日本医放会誌 1999 ; 59 : 745-749.
6) Swift PS : Carcinoma of Uterine Cervix. Textbook of Radiation Oncology. Leibel SA and Phillips TL ed, Philadelphia ; Saunders, 1998 : 820-823.
7) Brenner DJ et al : Conditions for the equivalence of continuous to plused low dose rate brachy therapy. Int J Radiat Oncol Biol Phys 1991 ; 20 : 181-190.
8) Martinez A et al : Combination of external beam irradiation and multiple-site perineal applicator (MUPIT) for treatment of locally advanced or recurrent prostatic, anorectal and gynecologic malignancies. Int J Radiat Oncol Biol phys 1985 ; 11 : 391-398.
9) Delgado G et al : Prospective surgical pathological study of disease free interval in patients with stage IB squamous cell carcinoma of the cervix : A Gynecologic Oncology Group Study. Gynecol Oncol 1990 ; 38 : 352-357.
10) Rotman M et al : Prophylactic extended field irradiation of para-aortic lymph nodes in stage IIB and bulky IB and IIA cervical carcinomas. Ten-year treatment results of RTOG 79-20. JAMA 1995 ; 274 : 387-393.
11) Special Issue : Late effects of normal tissue (LENT) consensus conference. Int Radiat Oncol Biol Phys 1995 ; 31(5) : whole book.
12) 荒居竜雄，他：子宮頸癌放射線治療による局所障害－低線量率および高線量率腔内照射の相違について－．癌の臨床 1976 ; 22 : 1417-1423.
13) Kupelian PA et al : Treatment of endometrial carcinoma whit radiation therapy alone. Int J Radiat Oncol Biol Phys 1993 ; 27 : 817-824.
14) Bruke TW et al : Gynecologic cancer : cancer of the uterine body. Cancer. Principles and Practices of Oncology, Ed. DeVita VT Jr et al, Philadelphia ; Lippincott-Raven, 1997 ; 1478-1499.
15) Carey MS et al : Good outcome associated with a standardized treatment protocol using selective postoperative radiation in patients with clinical stage I and adenocarcinoma of the endometrium. Gynecol Oncol 1995 ; 57 : 138-144.
16) Kadar N et al : Positive peritoneal cytology is an adverse factor in endometrial carcinoma only if there is evidence of extrauterine disease. Gynecol Oncol 1992 ; 46 : 145-149.
17) Green BE et al : Treatment of intraperitoneal metastatic adenocarcinoma of the

endometrium by the whole abdomen moving strip technique and pelvic boost irradiation. Gynecol Oncol 1983 ; 16 : 365 373.
18) Sears JD et al : Prognostic factors and treatment outcome for patients with locally recurrent endometrial cancer. Cancer 1994 ; 4 : 1303-1308.
19) Lanciano R et al : Update on the role of radiotherapy in ovarian cancer. Semin Oncol 1998 ; 5 : 361-371.
20) Dembo AJ : The ovary. Radiation Oncology, 6 th ed, Ed Moss WT & Cox JD, St. Louis ; Mosby, 1989 ; 586-593.
21) Fyles AW et al : Analysis of complications in patients with abdominopelvic radiation therapy for ovarian carcinoma. Int J Radit Oncol Biol phys 1992 ; 22 : 847-851.
22) Perez CA et al : Vagina. *Principles and Practice of Radiation Oncology*, 3 rd ed, Philadelphia ; Lippincott-Raven, 1997 ; 1891-1914.
23) Davis KP et al : Invasive vaginal carcinoma : analysis of early-stage disease. Gynecol Oncol 1991 ; 42 : 131-136.
24) Ogino I et al : High-dose-rate intracavitary brachytherapy in the management of cervical and vaginal intraepithelial neoplasia. Int J Radiat Oncol Biol Phys 1998 ; 40 : 881-887.
25) Stock RG et al : The importance of brachytherapy technique in the management of primary carcinoma of the vagina. Int J Radiat Oncol Biol Phys 1992 ; 24 : 747-753.
26) de Pree C et al : Feasibility and tolerance of pulsed dose rate interstitial brachytherapy. Int J Radiat Oncol Biol Phys 1999 ; 43 : 971-976.
27) Homesley HD et al : Radiation therapy versus pelvic node resection for carcinoma of the vulva with positive groin nodes. Obstet Gynecol 1986 : 68 ; 733-740.
28) Eifel PJ et al : Prolonged continuous infusion cisplatin and 5-fluorouracil with radiation for locally advanced carcinoma of the vulva. Gynecol Oncol 1995 ; 59 : 51-56.

コラム

hyperthermia

hyperthermia(温熱療法)は，41～45°C(特に 42.5°C 以上)で殺細胞効果があること，一般に腫瘍組織が熱感受性が高いこと，正常組織より血流の少ない腫瘍組織の方が加温されやすいことから癌の治療に有効とされる。また，hyperthermia は細胞周期からみて概ね放射線感受性の低い時期の細胞に高感受性で，41°C 以上で放射線の効果を増強するため，放射線療法と併用されることが多い。種々の抗癌薬の効果を増強するため，化学療法とも併用される。加温方法には，外部加温(表在加温と深部加温)，腔内加温，組織内加温があり，外部加温にはマイクロ波加温，RF(高周波)誘電加温が用いられている。表在加温は軟部組織腫瘍，頸部リンパ節転移などに，深部加温は胸壁浸潤型肺癌，骨盤部腫瘍などに，腔内加温は食道癌などに用いられる。治療の際には，腫瘍および周囲正常組織の温度を経時的に測定し，腫瘍全体を 42.5°C 以上とすることが望ましい。通常，その日の放射線治療後可能な限り速く開始して 30～60 分，週 1～2 回施行する。多くの比較臨床試験で，hyperthermia 併用放射線治療が放射線単独の治療成績を上回る結果が報告されている。

(栗林 徹)

Diffusion-Weighted Imaging of Prostate Cancer

Ryota Shimofusa, MD, Hajime Fujimoto, MD,† Hajime Akamata, MD,† Ken Motoori, MD,* Seiji Yamamoto, MD,* Takuya Ueda, MD,* and Hisao Ito, MD**

Objective: The purpose of this study was to assess whether T2-weighted (T2W) imaging with diffusion-weighted (DW) imaging could improve prostate cancer detection as compared with T2W imaging alone.

Methods: The subjects consisted of 37 patients with prostate cancer and 23 without cancer undergoing magnetic resonance (MR) imaging. Using a 1.5-T superconducting magnet, all patients underwent T2W and DW imaging with parallel imaging. Images were independently reviewed by 3 readers to determine the detectability of prostate cancer. The detectability of T2W imaging without and with DW imaging was assessed by means of receiver operating characteristic analysis.

Results: Mean areas under the receiver operating characteristic curve for T2W imaging alone and for T2W imaging with DW imaging were 0.87 and 0.93, respectively. The receiver operating characteristic analysis showed that the addition of DW imaging to conventional T2W imaging significantly improved tumor detection ($P = 0.0468$) compared with T2W imaging alone.

Conclusions: The addition of DW imaging to conventional T2W imaging provides better detection of prostate cancer.

Key Words: magnetic resonance imaging, prostate cancer, diffusion-weighted imaging, parallel imaging

(*J Comput Assist Tomogr* 2005;29:149–153)

The latest estimates of global cancer incidence show that prostate cancer is the third most common cancer in men, with half a million new cases each year.[1] In Japan, mortality attributable to prostate cancer is lower than in Western countries but is increasing rapidly.[1,2] Early detection of prostate cancer is vital for reducing mortality.

Recent reports have demonstrated the detectability of prostate cancer by magnetic resonance (MR) imaging.[3,4] On T2-weighted (T2W) imaging, regions of prostate cancer show decreased signal intensity relative to normal peripheral zone tissue because of increased cell density and a loss of prostatic ducts.[4] This finding is nonspecific, however, because other diseases such as prostatitis or hyperplasia can also cause low signal intensity on T2W imaging.[5–8] Moreover, detection of prostate cancer in the transition zone, which is present in up to 30% of all prostate cancer, is difficult because this zone is the site of the origin of benign prostatic hyperplasia, which can have a heterogeneous appearance.[9]

Recently, diffusion-weighted (DW) imaging has been available for abdominal and pelvic lesions such as liver,[10,11] renal,[12] and ovarian tumors.[13,14] Some preliminary studies[15–17] have indicated that DW imaging can differentiate a malignant neoplasm from benign prostate tissue because of a significant difference in the apparent diffusion coefficient value. These studies did not evaluate the ability to detect human prostate cancer, however.

When obtaining DW images, susceptibility artifacts on echo planar imaging sequences often degrade the quality of images. This was the principal problem when obtaining DW images of the prostate, which is located adjacent to stool and gas in the rectum. With a recent technical evolution, a parallel imaging technique (sensitivity encoding [SENSE]) is now available, however. Using SENSE, less distorted DW images of human prostate are available, because susceptibility artifacts can be significantly reduced.[18] The purpose of this study was to determine the detectability of prostate cancer by T2W imaging with DW imaging as compared with T2W imaging alone.

MATERIALS AND METHODS

Patients

This was a retrospective study conducted at a single institution. Between February and November 2003, 124 consecutive patients with clinically suspected prostate cancer because of elevated (>4.0 ng/mL) prostate specific antigen but with no prior treatment of prostate cancer underwent MR examination, including DW imaging. Sixty of the 124 patients had a histopathologic diagnosis proven by surgery or routine biopsy of 10 sites, including the central gland and peripheral zone. The other 64 patients were finally excluded from this study. Although a biopsy was planned for 30 of these 64 patients, it was not performed within the period of this study. The remaining 34 patients did not undergo biopsy at our institution because of 1) deterioration in general health (n = 12), 2) multiple metastatic disease (n = 5), 3) the patient's desire to be followed up without biopsy (n = 8), and 4) the patient's desire to consult another hospital (n = 9). The numbers of patients with surgically and biopsy-proven prostatic carcinoma were 18 and 19, respectively. Fourteen patients were free of malignancy on biopsy of 10 sites. Nine patients without cancer and undergoing transurethral resection because of symptoms of

Received for publication November 4, 2004; accepted January 6, 2005.
From the *Department of Radiology, Chiba University Hospital, Chiba, Japan; and †Department of Radiology, Numazu City Hospital, Shizuoka, Japan.
Reprints: Ryota Shimofusa, Department of Radiology, Chiba University Hospital, 1-8-1, Inohana, Chuo-ku, Chiba City, Chiba, Japan, 260-8677 (e-mail: mofu@indigo.plala.or.jp).

benign prostatic hyperplasia were also included. Overall, 37 (62%) of the 60 patients had prostate cancer. These patients underwent biopsy and/or surgery within 6 months after the MR examination. The mean patient age was 71 years (range: 54–82 years), and the mean prostate specific antigen value was 21.8 ng/mL (range: 4.5–130 ng/mL). Informed consent was obtained from all patients before MR imaging.

Imaging Protocol

Magnetic resonance images were obtained with a 1.5-T MR imaging system (Gyroscan Intera; Philips Medical Systems, Best, The Netherlands). We used a 4-channel pelvic phased-array coil. All patients underwent DW imaging in addition to imaging using a routine prostatic MR protocol. This routine protocol included transverse, sagittal, and coronal T2W fast spin echo sequences (3800–4000 milliseconds/120 milliseconds repetition time/echo time, 20-cm × 20-cm field of view, 256–280 × 512 matrix, echo train length = 16, 3–4-mm slice thickness, 0.5-mm intersection gap, average of 2).

Axial DW images were obtained by the single-shot echo planar imaging technique using the following imaging parameters: 2500 milliseconds/90 milliseconds repetition time/echo time, 20-cm × 20-cm field of view, 128 × 128 matrix, 3–4-mm slice thickness, 0.5-mm intersection gap, average of 2. Isotropic DW images were obtained by using diffusion gradients with 2 b-values (0 and 1000 sec/mm^2) along 3 directions of motion-probing gradients. We used a SENSE reduction factor of 2. The SENSE reduction factor is the ratio between the number of phase-encoding steps required for full-Fourier imaging and the number of phase-encoding steps necessary for an accelerated SENSE scan.

Image Analysis

Images were interpreted by 3 readers (R.S., H.F., and H.A.) blinded to the results of biopsy or operation.

At first, T2W images alone were interpreted without knowledge of the results of DW imaging. The criterion for detecting prostatic cancer was a low-intensity mass relative to high-intensity background of the normal peripheral zone.[4] On the basis of the findings, the presence or absence of prostate cancer was estimated by the readers using a 5-point rating scale (definitely or almost definitely present = 5, probably present = 4, possibly present = 3, probably absent = 2, and definitely or almost definitely absent = 1). On T2W imaging, we also assessed the presence or absence of benign prostatic hyperplasia.

More than 2 weeks after the first reading, the 3 readers reviewed combined T2W and DW imaging. Because anatomic detail was unclear as the result of a low signal-to-noise ratio on DW images, we referred to axial T2W images of the same planes. We determined the diagnostic criteria of DW imaging as follows: focal hyperintense (relative to background prostatic structure) lesions almost definitely present received a score of 5, focal hyperintense lesions probably present received a score of 4, focal hyperintense lesions possibly present received a score of 3, focal hyperintense lesions probably absent received a score of 2, and focal hyperintense lesions almost definitely absent received a score of 1. These criteria were applied to all prostatic regions, including the central gland.

For the calculation of sensitivity and specificity, these results were dichotomized so that scores of 1 through 3 were rated as cancer absent and scores of 4 and 5 were rated as cancer present.

Statistical Analysis

Receiver operating characteristic analysis was used to compare the results of routine T2W imaging alone and T2W imaging combined with DW imaging (rating scale range: 1–5). The area under the receiver operating characteristic curve (Az) was calculated for each reader and MR sequence. The statistical significance ($P < 0.05$) of differences in the Az was determined by means of the unpaired Student t test. Receiver operating characteristic curves were estimated with the ROCKIT 0.9B beta version program (C. Metz, Chicago, IL). Sensitivity, specificity, positive predictive value, and negative predictive value were also calculated.

RESULTS

The Az values, sensitivity, specificity, positive predictive value, and negative predictive value of the 3 readers are summarized in Table 1. All readers achieved higher sensitivity and specificity on combined T2W and DW imaging than on T2W imaging alone.

The Az values for the 3 readers for each T2W imaging and T2W imaging combined with DW imaging were 0.85 versus 0.93, 0.88 versus 0.96, and 0.87 versus 0.89, respectively. The mean Az value for each T2W imaging and combined T2W and DW imaging was 0.87 versus 0.93 (Fig. 1). Receiver operating characteristic analysis revealed that the addition of DW imaging to T2W imaging improved the diagnostic performance significantly ($P = 0.0468$). There were no significant differences in diagnostic accuracy among the 3 readers ($P > 0.05$).

Diffusion-weighted imaging clearly depicted prostate cancer as focal hyperintense areas (Figs. 2, 3). With the enhanced contrast between cancer and other prostatic tissue, T2W imaging with DW imaging resulted in a total 96 (86%) of

TABLE 1. Diagnostic Performance of T2W Imaging Alone and Combined T2W and DW Imaging for the Detection of Prostate Cancer

	Sensitivity (%)	Specificity (%)	Positive Predictive Value (%)	Negative Predictive Value (%)	Az
T2W imaging alone					
Reader 1	76	74	82	65	0.85
Reader 2	73	83	87	66	0.88
Reader 3	86	74	84	77	0.87
Mean	78	77	84	69	0.87
Combined T2W and DW imaging					
Reader 1	84	83	89	76	0.93
Reader 2	86	91	94	81	0.96
Reader 3	89	78	87	82	0.89
Mean	86	84	90	79	0.93

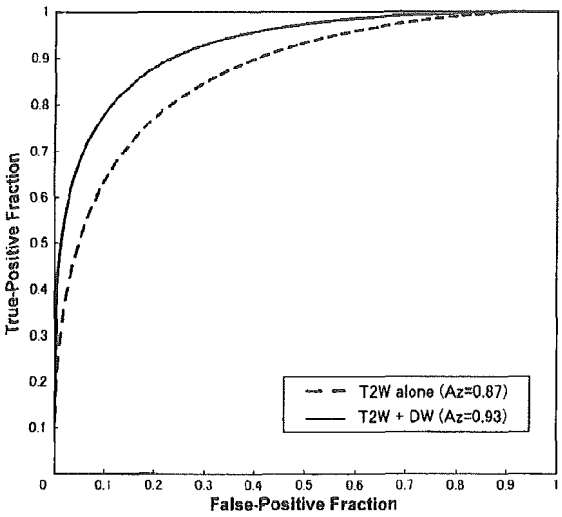

FIGURE 1. Mean receiver operating characteristic curves compare the performance of T2-weighted (T2W) imaging alone and combined T2W and diffusion-weighted (DW) imaging for detection of prostate cancer. The mean areas under the receiver operating characteristic curves (Az) of T2W imaging alone and combined T2W and DW imaging are 0.87 and 0.93, respectively. The difference between the 2 receiver operating characteristic curves is significant ($P = 0.0468$).

111 (31 of 37 cases for reader 1, 32 of 37 cases for reader 2, and 33 of 37 cases for reader 3) reviewed cancerous cases being judged as positive, although with T2W imaging alone, 87 (78%) of the 111 (28 of 37 cases for reader 1, 27 of 37 cases for reader 2, and 32 of 37 cases for reader 3) reviewed cancerous cases were judged as positive. In addition, DW imaging might assist in detecting prostate cancer involving the transition zone, which is difficult to discriminate from other lesions such as benign prostatic hyperplasia on T2W imaging alone (see Fig. 3). Radical prostatectomy specimens demonstrated that 8 of 18 patients had cancer foci involving the transition zone. Diffusion-weighted imaging distinctly depicted the cancer in the transition zone as hyperintense (score 4 or 5 by all readers) in 5 (63%) of the 8 patients. On T2W imaging alone, however, cancer in the transition zone could be clearly identified only in 1 (13%) of the 8 patients. This 1 patient had a cancer focus continuum involving the peripheral zone to the transition zone.

Diffusion-weighted imaging could differentiate between prostate cancer and some nonspecific hypointense lesions mimicking cancer on T2W imaging (Fig. 4). Of the total 180 (3 readers with 60 cases each) reviewed cases, there were 16 false-positive cases with T2W imaging alone, a number reduced to 11 cases with DW imaging. All readers also achieved a higher negative predictive value on combined T2W and DW imaging than on T2W imaging alone. Mean negative predictive values for T2W imaging alone and T2W with DW imaging were 69% and 79%, respectively.

DISCUSSION

Magnetic resonance imaging is widely used for determination of prostatic disease. Because of the similarity in signal intensity between prostate cancer and other benign lesions such as benign prostatic hyperplasia on T2W imaging, however, conventional MR imaging has good sensitivity (78%–83%) but low specificity (50%–55%) in detecting and localizing prostate cancer.[4–9] Additional procedures, such as MR spectroscopy, have been applied to achieve a more specific diagnosis and localization of prostate cancer.[19,20] Combined MR imaging and spectroscopy indicated the presence of tumor with high sensitivity (95%) and high specificity (91%).[20] Magnetic resonance spectroscopy is not routinely used with commercially available MR systems, however. Some reports suggest that dynamic contrast-enhanced MR imaging can discriminate prostate cancer from normal prostatic tissue.[21] The reported sensitivity (74%) and specificity (81%) of the dynamic contrast-enhanced study for tumor detection are lower than those of MR spectroscopy, however, and are not significantly different from the values of conventional fast spin echo images.[21]

Diffusion-weighted imaging offers another solution for identifying cancer in the prostate. Because of the many tightly packed glandular elements with little central space for mucin or fluid storage in prostate cancer, apparent diffusion

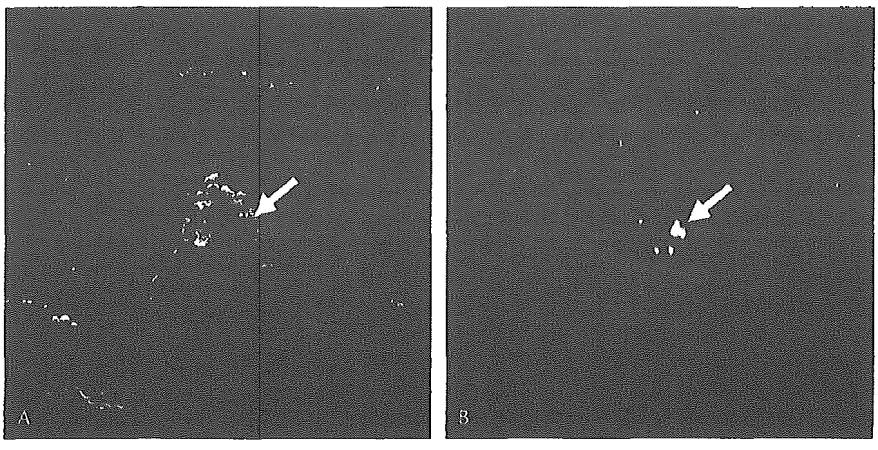

FIGURE 2. Prostate cancer in a 63-year-old man. A, Axial T2-weighted fast spin echo image (4000 milliseconds/120 milliseconds repetition time/echo time) shows a 15-mm diameter hypointense tumor (arrow) in the left peripheral zone. B, Axial imaging–diffusion-weighted image of the same plane reveals a focal hyperintense tumor (arrow). A radical prostatectomy specimen revealed moderately differentiated adenocarcinoma.

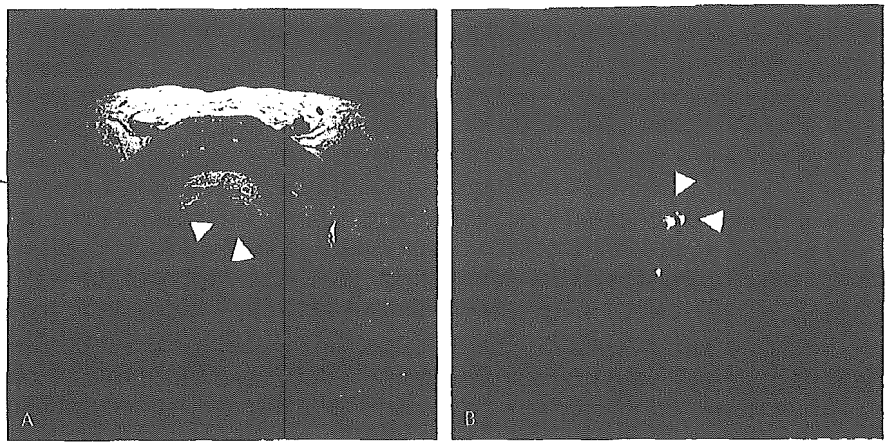

FIGURE 3. Prostate cancer in a 72-year-old man. A, Axial T2-weighted image (3880 milliseconds/120 milliseconds repetition time/echo time) shows a 20-mm diameter hypointense area in the left central gland (arrowheads). Discrimination of prostate cancer from other benign lesions, such as a benign prostatic hyperplastic nodule, is difficult. B, Axial imaging–diffusion-weighted image of the same plane clearly demonstrates a focal hyperintense lesion (arrowheads). A radical prostatectomy specimen revealed moderately differentiated adenocarcinoma.

coefficient values, which correspond to the restriction of water displacement, are reportedly significantly lower than in normal prostate.[16] Compared with MR spectroscopy, pelvic DW imaging is more easily performed on most MR scanners without additional software, although every system has several limitations. Without parallel imaging, however, DW imaging of the prostate is not performed as part of routine clinical MR imaging, mainly because of susceptibility artifacts that degrade the image and make it difficult to localize the tumor. Applying parallel imaging, the accumulating phase that causes susceptibility artifacts is decreased because of a reduction in the train of gradient echoes and sampling time. Shortened imaging times with parallel imaging also contribute to the suppression of motion artifacts.

To our knowledge, this is the first clinical study to apply DW imaging with parallel imaging and with a high b-value (b = 1000) to the detection of prostate cancer. On DW imaging, prostate cancer was depicted as a hyperintense focal lesion with markedly enhanced contrast compared with T2W imaging (see Fig. 2). Therefore, we could differentiate cancers from noncancerous lesions with greater confidence. In addition, DW imaging has the capability of revealing prostate cancer not only in the peripheral zone but in the transition zone (see Fig. 3). The capability of detecting cancer in the transition zone gives DW imaging a great advantage over conventional T2W imaging and MR spectroscopic imaging. The result of higher performance in the detection of prostate cancer was particularly related to this capability. Although there were differences in the patient populations, sensitivity (86%) and specificity (84%) on T2W imaging with DW imaging in our study without an endorectal coil were higher than those of former studies (sensitivity: 74%–83%, specificity: 50%–81%) with an endorectal coil[4–9] and a dynamic study.[21]

The apparent diffusion coefficient value was not quantified in the present study. Because we used a high b-value (b = 1000) to enhance the contrast between normal and cancerous prostate, the signal-to-noise ratio was reduced and an adequate region of interest was not ensured in correlation with the pathologic specimen in the present study. This is usually the case for small lesions. Regardless of whether the precise apparent diffusion coefficient value is calculated or not, b-values of 400 to 500 as used in liver DW imaging[10,11] may be more appropriate for a balance between the signal-to-noise ratio and diffusion weighting. Even when using high b-values, it might be possible to improve the signal-to-noise ratio with increased averaging[15] and/or with the use of an endorectal coil modified for echo planar imaging by being inflated with liquid.[17] The most appropriate b-value for DW imaging of the prostate is

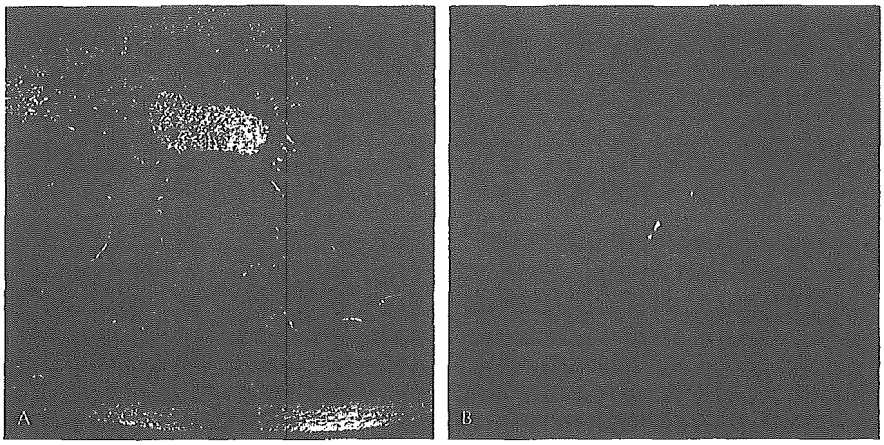

FIGURE 4. A 72-year-old man without prostate cancer. A, Axial T2-weighted image (3900 milliseconds/120 milliseconds repetition time/echo time) shows an enlarged prostatic gland as a result of benign prostatic hyperplasia. A small hypointense focus is detected in the left peripheral zone (arrow). Prostate cancer cannot be excluded on the basis of this appearance. B, Axial diffusion-weighted image of the same plane demonstrates no focal hyperintense lesion relative to other regions of the prostate. Biopsies of 10 sites, including the left peripheral zone, did not reveal a malignant focus.

still to be established. Further studies with various b-values, larger patient populations, and imaging sequence modifications are needed.

In conclusion, our results demonstrate the potential value of prostatic DW imaging in clinical practice. Diffusion-weighted imaging combined with T2W imaging provides a higher detection rate of prostate cancer.

REFERENCES

1. Quinn M, Babb P. Patterns and trends in prostate cancer incidence, survival, prevalence and mortality. Part I: international comparisons. *BJU Int.* 2002;90:162–173.
2. Quinn M, Babb P. Patterns and trends in prostate cancer incidence, survival, prevalence and mortality. Part II: individual countries. *BJU Int.* 2002;90:174–184.
3. Thornbury JR, Ornstein DK, Choyke PL, et al. Prostate cancer: what is the future role for imaging? *AJR Am J Roentgenol.* 2001;176:17–22.
4. Yu KK, Hricak H. Imaging prostate cancer. *Radiol Clin N Am.* 2000; 38:59–85.
5. Hricak H, White S, Vigneron D, et al. Carcinoma of the prostate gland: MR imaging with pelvic phased-array coils versus integrated endorectal-pelvic phased-array coils. *Radiology.* 1994;193:703–709.
6. Quint LE, Van Erp JS, Bland PH, et al. Prostate cancer: correlation of MR images with tissue optical density at pathologic examination. *Radiology.* 1991;179:837–842.
7. Lovett K, Rifkin MD, McCue PA, et al. MR imaging characteristics of noncancerous lesions of the prostate. *J Magn Reson Imaging.* 1992;2: 35–39.
8. White S, Hricak H, Forstner R, et al. Prostate cancer: effect of postbiopsy hemorrhage on interpretation of MR images. *Radiology.* 1995;195:385–390.
9. Ikonen S, Kivisaari L, Tervahartiala P, et al. Prostatic MR imaging. Accuracy in differentiating cancer from other prostatic disorders. *Acta Radiol.* 2001;42:348–354.
10. Namimoto T, Yamashita Y, Sumi S, et al. Focal liver masses: characterization with diffusion-weighted echo-planar MR imaging. *Radiology.* 1997;204:739–744.
11. Ichikawa T, Haradome H, Hachiya J, et al. Diffusion-weighted MR imaging with a single-shot echoplanar sequence: detection and characterization of focal hepatic lesions. *AJR Am J Roentgenol.* 1998;170:397–402.
12. Squillaci E, Manenti G, Di Stefano F, et al. Diffusion-weighted MR imaging in the evaluation of renal tumours. *J Exp Clin Cancer Res.* 2004;23:39–45.
13. Moteki T, Ishizaka H. Diffusion-weighted EPI of cystic ovarian lesions: evaluation of cystic contents using apparent diffusion coefficients. *J Magn Reson Imaging.* 2000;12:1014–1019.
14. Katayama M, Masui T, Kobayashi S, et al. Diffusion-weighted echo planar imaging of ovarian tumors: is it useful to measure apparent diffusion coefficients? *J Comput Assist Tomogr.* 2002;26:250–256.
15. Gibbs P, Tozer DJ, Liney GP, et al. Comparison of quantitative T2 mapping and diffusion-weighted imaging in the normal and pathologic prostate. *Magn Reson Med.* 2001;46:1054 1058.
16. Song SK, Qu Z, Garabedian EM, et al. Improved magnetic resonance imaging detection of prostate cancer in a transgenic mouse model. *Cancer Res.* 2002;62:1555–1558.
17. Issa B. in vivo measurement of the apparent diffusion coefficient in normal and malignant prostatic tissues using echo-planar imaging. *J Magn Reson Imaging.* 2002;16:196–200.
18. Bammer R, Keeling SL, Augustin M, et al. Improved diffusion-weighted single-shot echo-planar imaging (EPI) in stroke using sensitivity encoding (SENSE). *Magn Reson Med.* 2001;46:548–554.
19. Kurhanewicz J, Vigneron DB, Hricak H, et al. Three-dimensional H-1 MR spectroscopic imaging of the in situ human prostate with high (0.24–0.7-cm^3) spatial resolution. *Radiology.* 1996;198:795–805.
20. Scheidler J, Hricak H, Vigneron DB, et al. Prostate cancer: localization with three-dimensional proton MR spectroscopic imaging—clinicopathologic study. *Radiology.* 1999;213:473–480.
21. Jager GJ, Ruijter ET, van de Kaa CA, et al. Dynamic TurboFLASH subtraction technique for contrast-enhanced MR imaging of the prostate: correlation with histopathologic results. *Radiology.* 1997;203:645–652.

Diagnostic Value of FDG PET and Salivary Gland Scintigraphy for Parotid Tumors

Yoshitaka Uchida, MD, PhD, Satoshi Minoshima,† Tetsuya Kawata,* Ken Motoori,* Koichi Nakano,‡ Toshiki Kazama,§ Takashi Uno,* Yoshitaka Okamoto,‖ and Hisao Ito**

Purpose: The purpose of this study was to examine the diagnostic value of the combination of F-18 fluorodeoxyglucose (FDG) PET and Tc-99m pertechnetate salivary gland scintigraphy in parotid tumors.

Materials and Methods: Seventy-two patients with benign parotid gland tumors (n = 52), malignant parotid tumors (n = 12), and inflammation (n = 8) underwent both FDG PET and salivary gland scintigraphy within 1 week, and 66 of the patients also underwent gallium scintigraphy. All patients were negative on their first fine-needle aspiration (FNA).

Results: Malignant parotid tumors showed significantly higher FDG uptake (standard uptake values [SUVs]) than both benign tumors and inflammation, except in Warthin's tumor (5.82 ± 3.95 vs. 2.07 ± 1.33; $P < 0.01$). Although the SUV values of Warthin's tumor and malignant parotid tumors overlapped somewhat, Warthin's tumor did demonstrate increased radiotracer uptake, and it was reliably distinguished from other parotid gland tumors by the use of salivary gland scintigraphy. Considering a SUV value >3 as being positive for malignancy and excluding Warthin's tumor on the basis of salivary gland scintigraphy, sensitivity and specificity of FDG PET were 75% and 80%, respectively. These results were superior to those of gallium scintigraphy (58% and 72%, respectively).

Conclusions: Although the diagnostic value of FDG PET in the differentiation of malignant from benign parotid gland tumors was limited because of the high FDG uptake in some benign tumors, and particularly pleomorphic adenomas, combining salivary gland scintigraphy with FDG PET may help to negate this drawback, and this combination may be a more promising approach for differentiation of various parotid gland tumors in patients compared with nondiagnostic needle aspiration.

Key Words: parotid tumor, F-18 FDG PET, salivary grand scintigraphy, diagnosis, sensitivity

(*Clin Nucl Med* 2005;30: 170–176)

Identification of the different types of primary parotid tumors is essential for selecting among the various treatments—resection or preservation of the facial nerve, extended radical or superficial parotidectomy, and possibly additional radical neck dissection. Presurgical evaluation of primary parotid tumors relies on clinical and radiologic workup. Gallium-67 scintigraphy, sialograms, computed tomography (CT), and magnetic resonance imaging (MRI) have all been used in the diagnosis of parotid tumors, but they are not necessarily specific to the types of tumors.[1,2] Fine-needle aspiration (FNA) is also commonly used, but its accuracy (sensitivity and specificity) is not so consistent and is also considered to possibly be responsible for postresection recurrence.[3,4] Alternative methods are desired for better presurgical evaluation of parotid tumors.

Positron emission tomography (PET) with F-18 fluorodeoxyglucose (FDG) has been used for diagnosing malignant tumors of various regions.[5–7] A few investigators previously reported that the use of FDG PET in the evaluation of parotid tumors is limited because of a relatively high false-positive rate (approximately 30%).[8] In a previous study, however, we found that a common cause of false-positives is the high FDG uptake in Warthin's tumors.[9] Because it is known that Warthin's tumors tend to show increased radiotracer uptake on salivary gland scintigraphy[10] as well, we hypothesized that a combination of FDG PET and salivary gland scintigraphy would better characterize parotid tumors. The present study was conducted prospectively to examine the diagnostic value of FDG PET and salivary gland scintigraphy in parotid tumors, including a comparison with gallium scintigraphy.

Received for publication August 7, 2004. Revision accepted October 24, 2004.

From the **Departments of Radiology, Chiba University School of Medicine, Chiba, Japan; the †Department of Radiology, University of Washington School of Medicine, Seattle, Washington; the ‡Department of Otolaryngology, Chiba Aoba Municipal Hospital, Chiba, Japan; the §Department of Radiology, Numazu Municipal Hospital, Shizuoka, Japan; and the ‖Department of Otolaryngology, Chiba University School of Medicine, Chiba, Japan.

Reprints: Yoshitaka Uchida, MD, PhD, Department of Radiology, Chiba University School of Medicine, 1-8-1 Inohana, Chuuou-ku, Chiba-shi, Chiba 260-8677, Japan. E-mail: uchiday@faculty.chiba-u.jp.

ISSN: 0363-9762/05/3003-0170

MATERIALS AND METHODS

Seventy-two patients with benign parotid tumors (n = 52), primary malignant parotid tumors (n = 12), and inflammation (n = 8) were recruited in this study. All patients had a negative diagnosis on their first FNA. The patients consisted of 33 females and 39 males (mean age, 52 years; range, 10–84 years). Salivary gland scintigraphy was performed on all patients, and 66 patients also underwent gallium scintigraphy. The diagnoses of all patients were confirmed histopathologically (Table 1). Informed consent was obtained from all patients before PET scanning.

F-18 and FDG were synthesized using a CYPRIS and CUPID system (Sumitomo Heavy Industry, Tokyo, Japan). PET imaging was performed with a SET-110W (Shimadzu, Kyoto, Japan). All patients fasted for at least 6 hours before the procedure. A transmission scan was performed and used for attenuation correction. FDG PET images were obtained 60 minutes after intravenous injection of 185 MBq (5mCi) FDG. Nine slices, each 5.5 mm thick, were acquired simultaneously. PET slice levels were determined according to a skin marker placed over the tumor under ultrasonographic guidance. The in-plane spatial resolution of reconstructed PET images was 10.4 mm FWHM. Regions-of-interest (ROIs) were placed on PET images at the peak of tumor uptake. Tumor uptake was identified by a comparison with ultrasonographic findings and MRI images. Metabolic activity was converted to a standard uptake value (SUV) according to the formula for body weight by dividing tissue volume (MBq/mL) by activity injected per body weight (MBq/g). Student *t* test was used to assess differences in FDG uptake among tumors.

Salivary gland scintigraphy and gallium scintigraphy were performed using a PRISM 2000 camera (Shimadzu). Images were obtained after intravenous injection of 185 MBq (5 mCi) Tc-99m sodium pertechnetate or 111 MBq (3 mCi) gallium-67 citrate. Salivary gland scintigraphy was obtained with both pre- and postoral citric acid stimulation. Tumor uptake in the 2 scintigraphies was interpreted visually.

TABLE 1. Histopathologic confirmation of parotid tumors

Adenoid cystic carcinoma	3
Adenocarcinoma	3
Salivary duct carcinoma	2
Undifferentiated carcinoma	1
Squamous cell carcinoma	1
Mucoepidermoid carcinoma	1
Renal cell carcinoma (meta)	1
Pleomorphic adenoma	20
Warthin's tumor	14
Basal cell adenoma	4
Lymphoepithelial cyst	3
Follicular hyperplasia	2
Eosinophilic granuloma	2
Lymphangioma	2
Bronchogenic cyst	1
Ductal cyst	1
Monomorphic adenoma	1
Atypical lymphocyte	1
Oncocytoma	1
Inflammation	8

RESULTS

The mean SUV of malignant parotid tumors was significantly greater than that of benign tumors when excluding Warthin's tumors from the analysis (5.82 ± 3.95 vs. 2.07 ± 1.33; $P < 0.01$). The SUV of Warthin's tumor was greater than that of other benign tumors (7.06 ± 3.99 vs. 2.07 ± 1.33; $P < 0.001$) and overlapped with that of malignant tumors (Fig. 1).

On salivary gland scintigraphy, all Warthin's tumors and 1 oncocytoma showed retention of Tc-99m sodium pertechnetate after oral acid stimulation. Because other parotid gland tumors in this study showed cold defects or were equivocal on salivary gland scintigraphy, we could distinguish Warthin's tumor and oncocytoma from other parotid gland tumors.

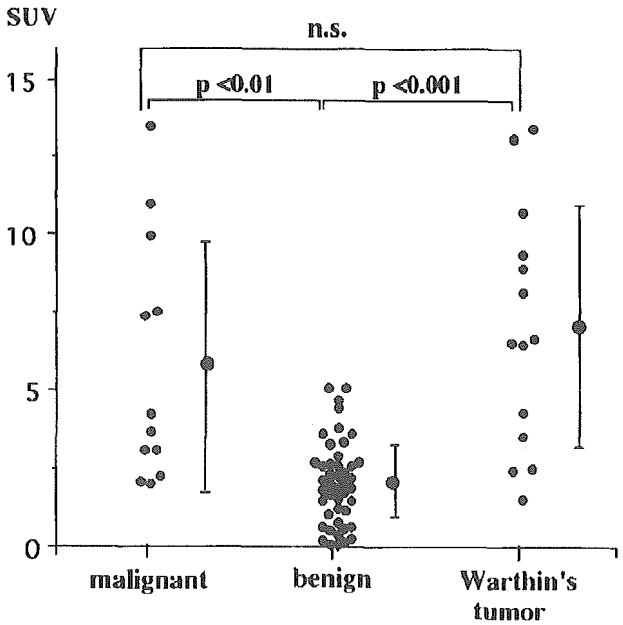

FIGURE 1. SUV of FDG in parotid tumors. A mean SUV of malignant parotid tumors was significantly greater than that of benign tumors, except Warthin's tumor. SUV of Warthin's tumor was greater than that of other benign tumors and overlapped with that of malignant tumors.

When excluding Warthin's tumors and oncocytoma based on salivary gland scintigraphic findings and then considering an SUV above 3 as "positive" for malignancy, sensitivity and specificity of FDG PET were 75% and 80%, respectively (Table 2; Figs. 2 and 3). False-negative cases were found in 1 salivary duct carcinoma (SUV 2.01), 1 mucoepidermoid carcinoma (SUV 2.07), and 1 metastatic tumor of renal cell carcinoma (SUV 2.24). Tumor size of all false-negative cases was small (10 mm, 17 mm, and 20 mm, respectively). False-positives were found in 5 pleomorphic adenomas (Fig. 4), 2 inflammations, 1 basal cell adenoma, and 1 monomorphic adenoma.

By visual interpretation, sensitivity (58%) and specificity (72%) of Ga-67 scintigraphy were inferior to FDG PET (Table 2). False-negatives were found in 2 adenoid cystic carcinomas, 1 salivary duct carcinoma, 1 adenocarcinoma, and 1 undifferentiated carcinoma. False-positives were found in 4 pleomorphic adenomas, 4 inflammations, 1 basal cell adenoma, 1 lymphoepithelial cyst, 1 atypical lymphocyte, and 1 monomorphic adenoma.

Mean tumor size measured by ultrasonography (US) did not differ significantly among malignant (26 ± 9 mm), Warthin's (27 ± 6 mm), and other benign (23 ± 11 mm) tumors in this study.

DISCUSSION

Parotid tumors are not rare. Preoperative distinction between malignant and benign tumors is important clinically for surgical planning in terms of the possible necessity for resection of lymph nodes and the facial nerve. However, none of the physical examination findings, FNA, laboratory data, sialography, gallium scan, CT, US, or MRI is necessarily specific to the histopathology of parotid tumors.

All patients had a negative diagnosis on their first FNA in this study. FNA is cost-effective compared with imaging studies, and it can be performed without many complications. Recent studies have reported that the sensitivity of FNA is 64% to 92% and the specificity 75% to 100%.[3,11–13] However, there have been some disadvantages reported concerning FNA. The accuracy of FNA depends on the location of the tumor, tumor size, and the experience of physicians and cytopathologists. Therefore, a tumor may not always be benign when the results of FNA show no malignancy. In addition, there is agreement that enucleation of parotid tumors, defined as opening the capsule of the tumor followed by repeat aspiration of its contents, can lead to a high recurrence rate.[4,14–16] Surgical exposure of the tumor or the tumor capsule, including FNA, also risks spillage and dramatically increases the risk of recurrence.[4,14–16]

Several studies have demonstrated the potential use of FDG PET in the evaluation of head and neck tumors. Jabour and colleagues[17] as well as Nowak and colleagues[18] demonstrated that PET was slightly more sensitive than MRI in the detection of both primary squamous cell tumors and nodal metastases. Adams and coworkers[19] revealed that PET has the highest sensitivity and specificity for detecting lymph node metastases of head and neck cancers in comparison to CT/MRI/US.

Recently, some studies have reported the usefulness of FDG PET for parotid glands.[20] Keyes and colleagues[8] as well as McGuirt and colleagues[21] reported a high sensitivity of FDG PET in the detection of malignant parotid tumors, but a relatively high false-positive rate (approximately 30%). Although the reason is not yet clear, a high FDG uptake in Warthin's tumor is in part responsible for a common cause of a relatively high false-positive rate by PET. In this study, 11 of 14 patients with Warthin's tumors showed increased FDG uptake (SUV >3), which could be misinterpreted as being a malignant tumor only by the use of PET. The sensitivity and specificity to differentiate malignant versus benign parotid tumors only with the use of PET were 75% and 67%, respectively. To improve the false-positive rate of FDG PET, the use of salivary gland scintigraphy before PET was found to be very useful. All patients with Warthin's tumors and oncocytomas in this study showed retention of Tc-99m sodium pertechnetate after oral acid stimulation. After exclud-

TABLE 2. Results of Tc-99m pertechnetate salivary gland scintigraphy, FDG PET, and gallium scintigraphy in parotid tumors

	Tc-99m pertechnetate salivary gland scintigraphy		FDG PET		Gallium scintigraphy‡	
	Positive	Negative	Positive†	Negative	Positive	Negative
Malignant tumor (n = 12)	0	12	9	3	7	5
Warthin's tumor and oncocytoma (n = 15)	15	0	11	4	1	10
Benign tumor*(n = 45)	0	45	9	36	12	31

*Excluding Warthin's tumor.
†SUV above 3 considered "positive."
‡Six patients (4 Warthin's tumors and 2 pleomorphic adenomas) did not have gallium scintigraphy performed.

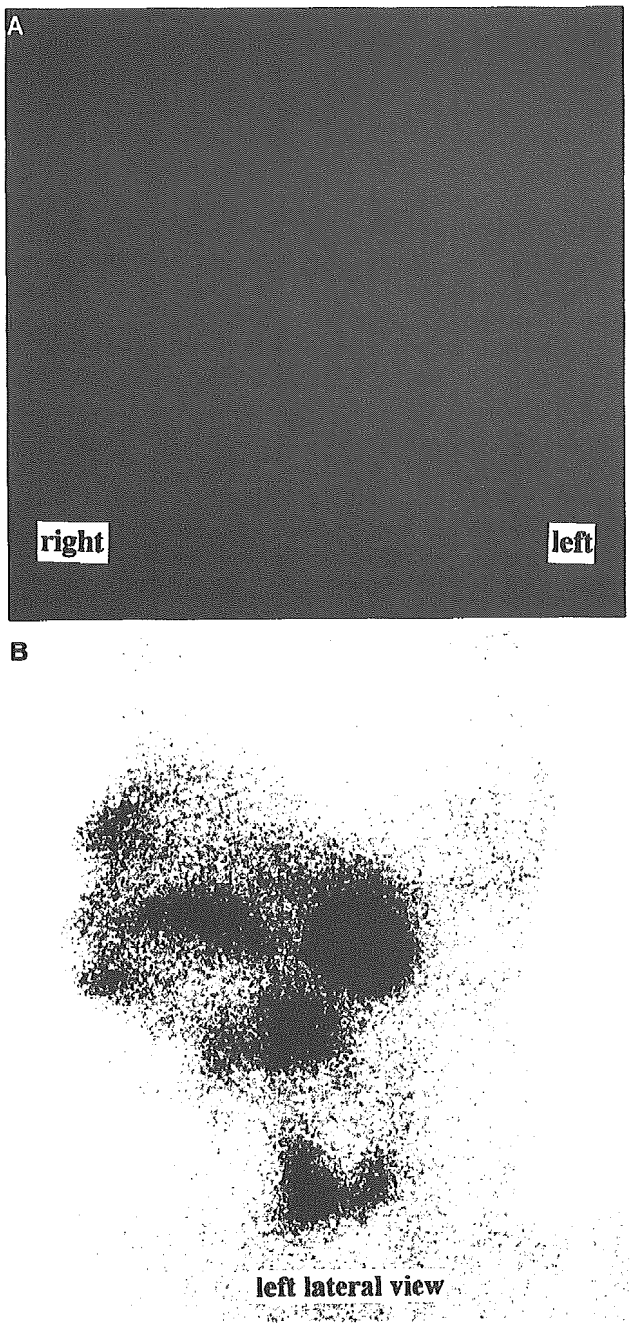

FIGURE 2. A 46-year-old woman with Warthin's tumor. (A) Increased FDG uptake in the tumor is seen, whereas (B) Tc-99m salivary gland scintigraphy (postoral citric acid stimulation) shows increased radioactivity. In this case, we could rule out malignancy by performing Tc-99m salivary gland scintigraphy first and avoid the false-positive result by FDG PET.

ing patients with Warthin's tumors and oncocytomas by salivary gland scintigraphy, the false-positive rate of FDG PET was lowered, and its diagnostic value was improved, ie, the specificity rising from 67% to 80%. No further examination is necessary for patients who are positive with salivary scintigraphy. However, for negative cases, FDG PET is essential in the in vivo noninvasive diagnostic workup for parotid tumors.

Specificity was still lower compared with that reported for FNA. The cause of the high false-positive rate in this study could be attributed to 5 cases (25%) of pleomorphic adenomas. The highest SUV rate of pleomorphic adenomas was 5.08, and their mean SUV was greater than that of other benign tumors and inflammation (2.33 ± 1.32 vs. 1.86 ± 1.32). Matsuda and coworkers reported that accumulation of FDG in patients with pleomorphic adenomas did not differ significantly among histologic types but did reflect tumor growth capacity.[22] Because most pleomorphic adenomas grow gradually, it appeared to be difficult to distinguish between malignant parotid tumors and pleomorphic adenomas completely only on the basis of FDG PET.

Sensitivity in this study was also lower compared with previous studies.[8,20,21] This may be attributed to the size of the tumors and metabolic activity. In all false-negative cases, tumor size was smaller than average size (26 mm) of malignant tumors and they were negative on the first FNA. Although 2 of the false-negative cases had a size above the resolution level of the equipment, their metabolic activity was too low to be detected. We considered these cases needed to have additional examinations performed such as dynamic MRI.[23]

Gallium scintigraphy is known to be useful in evaluating parotid gland tumors. In this study, the sensitivity and specificity of gallium scintigraphy were inferior to FDG PET. Two cases with high accumulation of FDG (adenocarcinoma and undifferentiated carcinoma) showed no accumulation by gallium scintigraphy, and there were 2 inflammation cases which were negative with FDG that had high accumulation on gallium scintigraphy. Because there is a difference between semiquantitative analysis and visual interpretation, if a nuclear medicine technique is deemed necessary for diagnosing a parotid tumor, we consider FDG PET to be superior to gallium scintigraphy.

CONCLUSIONS

To diagnose parotid tumors, Tc-99m pertechnetate salivary gland scintigraphy should be performed first for Warthin's tumor, which usually shows positive accumulation. In cases negative with Tc-99m, FDG PET should be performed as a next step to distinguish malignant from benign parotid tumors. It should be noted that some malignant tumors with small size or low metabolism can be false-negative and further studies are necessary to improve the specificity and sensitivity of FDG PET.

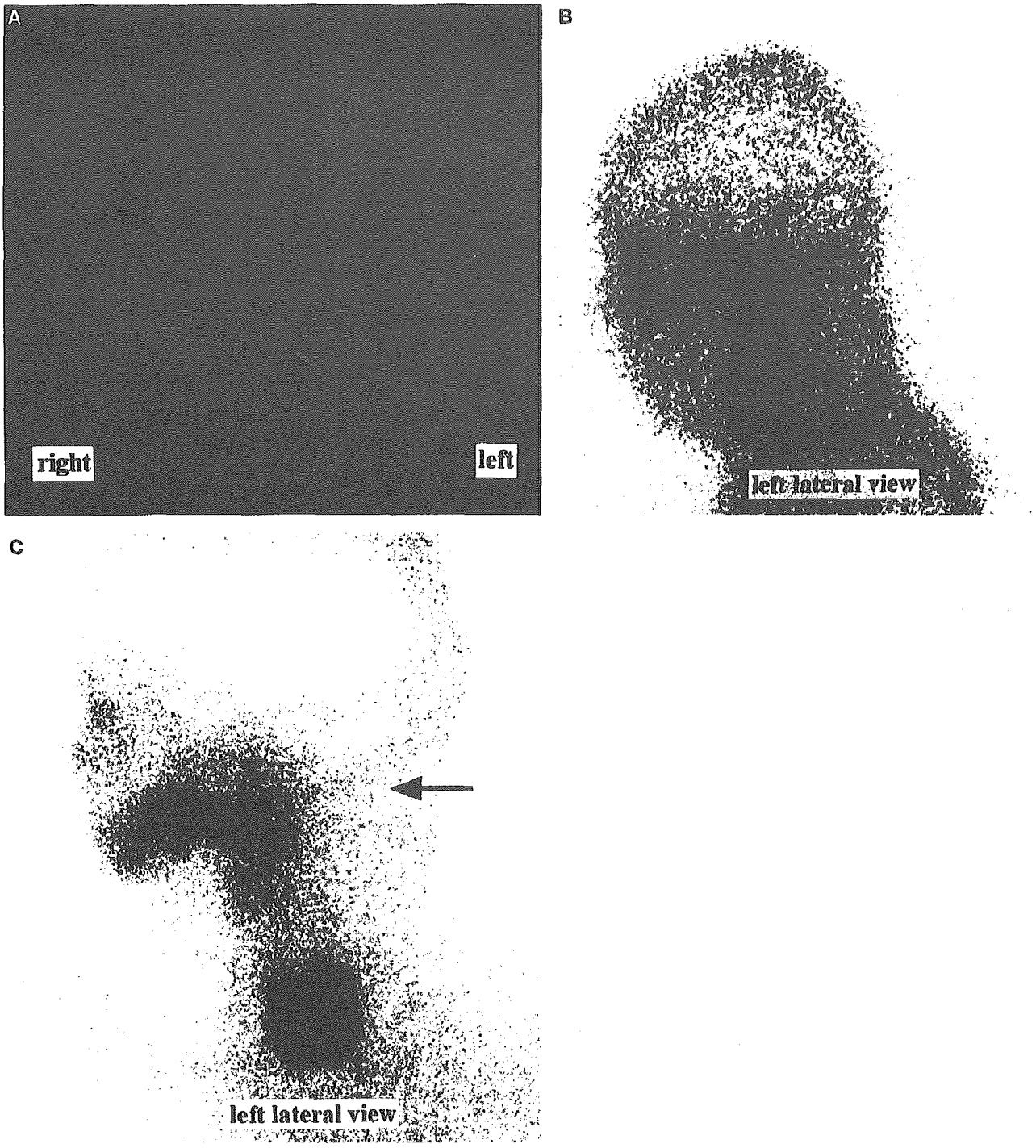

FIGURE 3. A 64-year-old man with squamous cell carcinoma. (A) There is increased FDG uptake in the tumor, and the SUV value is high (13.5). (B) No accumulation is seen on gallium scintigraphy, and (C) Tc-99m salivary scintigraphy (postoral citric acid stimulation) indicates a cold defect (arrow).

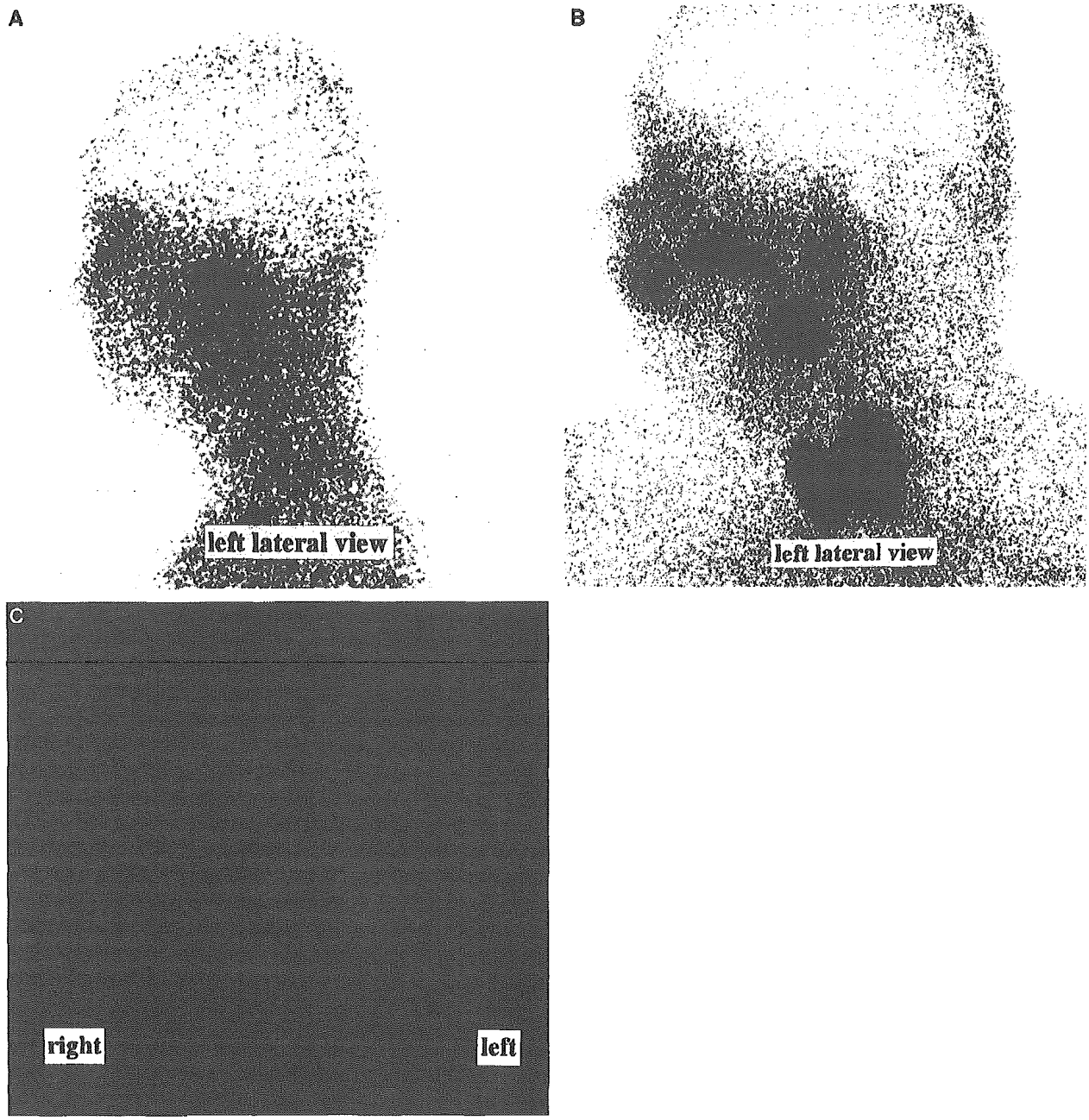

FIGURE 4. A 52-year-old man with pleomorphic adenoma. Both (A) gallium scintigraphy and (B) Tc-99m salivary scintigraphy show no accumulation. However, (C) increased FDG uptake in the tumor is seen and the SUV value is high (5.08).

REFERENCES

1. Shinohara S, Yamamoto E, Tanabe M, et al. Evaluation of RI scintiscanning to parotid gland tumors. *Nippon Jibiinkoka Gakkai Kaiho.* 2001;104:852–858.
2. Shah GV. MR imaging of salivary glands. *Magn Reson Imaging Clin North Am.* 2002;10:631–662.
3. Wong DS, Li GK. The role of fine-needle aspiration cytology in the management of parotid tumors: a critical clinical appraisal. *Head Neck.* 2000;22:469–473.
4. Touquet R, Mackenzie IJ, Carruth JA. Management of the parotid pleomorphic adenoma, the problem of exposing tumor tissue at operation. The logical pursuit of treatment policies. *Br J Oral Maxillofac Surg.* 1990;28:404–408.
5. Schiepers C, Filmont JE, Czernin J. PET for staging of Hodgkin's

disease and non-Hodgkin's lymphoma. *Eur J Nucl Med Mol Imaging*. 2003;30(suppl 1):S82–S88.
6. Pandit N, Gonen M, Krug L, et al. Prognostic value of [18F]FDG-PET imaging in small cell lung cancer. *Eur J Nucl Med Mol Imaging*. 2003;30:78–84.
7. Higashi T, Saga T, Nakamoto Y, et al. Diagnosis of pancreatic cancer using fluorine-18 fluorodeoxyglucose positron emission tomography (FDG PET)—usefulness and limitations in 'clinical reality'. *Ann Nucl Med*. 2003;17:261–279.
8. Keyes JW Jr, Harkness BA, Greven KM, et al. Salivary gland tumors: pretherapy evaluation with PET. *Radiology*. 1994;192:99–102.
9. Miyake H, Matsumoto A, Hori Y, et al. Warthin's tumor of parotid gland on Tc-99m pertechnetate scintigraphy with lemon juice stimulation: Tc-99m uptake, size, and pathologic correlation. *Eur Radiol*. 2001;11: 2472–2478.
10. Horiuchi M, Yasuda S, Shohtsu A, et al. Four cases of Warthin's tumor of the parotid gland detected with FDG PET. *Ann Nucl Med*. 1998;12: 47–50.
11. Stewart CJ, MacKenzie K, McGarry GW, et al. Fine-needle aspiration cytology of salivary gland: a review of 341 cases. *Diagn Cytopathol*. 2000;22:139–146.
12. Bartels S, Talbot JM, DiTomasso J, et al. The relative value of fine-needle aspiration and imaging in the preoperative evaluation of parotid masses. *Head Neck*. 2000;22:781–786.
13. Zbaren P, Schar C, Hotz MA, et al. Value of fine-needle aspiration cytology of parotid gland masses. *Laryngoscope*. 2001;111:1989–1992.
14. Donovan DT, Conley JJ. Capsular significance in parotid tumor surgery: reality and myths of lateral lobectomy. *Laryngoscope*. 1984;94:324–329.
15. Dykun RJ, Deitel M, Borowy ZJ, et al. Treatment of parotid neoplasms. *Can J Surg*. 1980;23:14–19.
16. Myssiorek D, Ruah CB, Hybels RL. Recurrent pleomorphic adenomas of the parotid gland. *Head Neck*. 1990;12:332–336.
17. Jabour BA, Choi Y, Hoh CK, et al. Extracranial head and neck: PET imaging with 2-[F-18]fluoro-2-deoxy-D-glucose and MR imaging correlation. *Radiology*. 1993;186:27–35.
18. Nowak B, Di Martino E, Janicke S, et al. Diagnostic evaluation of malignant head and neck cancer by F-18-FDG PET compared to CT/MRI. *Nuklearmedizin*. 1999;38:312–318.
19. Adams S, Baum RP, Stuckensen T, et al. Prospective comparison of 18F-FDG PET with conventional imaging modalities (CT, MRI, US) in lymph node staging of head and neck cancer. *Eur J Nucl Med*. 1998; 25:1255–1260.
20. Okamura T, Kawabe J, Koyama K, et al. Fluorine-18 fluorodeoxyglucose positron emission tomography imaging of parotid mass lesions. *Acta Otolaryngol Suppl*. 1998;538:209–213.
21. McGuirt WF, Keyes JW Jr, Greven KM, et al. Preoperative identification of benign versus malignant parotid masses: a comparative study including positron emission tomography. *Laryngoscope*. 1995;105:579–584.
22. Matsuda M, Sakamoto H, Okamura T, et al. Positron emission tomographic imaging of pleomorphic adenoma in the parotid gland. *Acta Otolaryngol Suppl*. 1998;538:214–220.
23. Motoori K, Yamamoto S, Ueda T, et al. Inter- and intratumoral variability in magnetic resonance imaging of pleomorphic adenoma: an attempt to interpret the variable magnetic resonance findings. *J Comput Assist Tomogr*. 2004;28:233–246.